Journal of Renewable Materials

Tech Science Press

DOI: 10.32604/jrm.2022.020204

ARTICLE

Determining the *in vitro* Anti-Aging Effect of the Characteristic Components from *Eucommia ulmoides*

Xuesong Wang[1,#], Zhihong Wang[1,2,#], Qiuling Yang[1], Sheng Peng[3] and Mijun Peng[1,*]

[1]Guangdong Provincial Key Laboratory of Chemical Measurement and Emergency Test Technology, Guangdong Provincial Engineering Research Center for Ambient Mass Spectrometry, Institute of Analysis, Guangdong Academy of Sciences (China National Analytical Center, Guangzhou), Guangzhou, 510070, China

[2]Guangdong Provincial Key Laboratory of Silviculture, Protection and Utilization, Guangdong Academy of Forestry, Guangzhou, 510520, China

[3]National & Local United Engineering Laboratory of Integrative Utilization Technology of *Eucommia ulmoides* Jishou University, Jishou, 427000, China

[*]Corresponding Author: Mijun Peng. Email: pengmj163@163.com

[#]These authors contributed equally to this work

Received: 10 November 2021 Accepted: 27 December 2021

ABSTRACT

To evaluate the potential anti-aging ability of *Eucommia ulmoides*, four characteristic components (chlorogenic acid, geniposidic acid, aucubin, quercetin) were selected to assess their effects on H_2O_2-induced oxidative damage model of human umbilical vein endothelial cell (HUVEC). Oxidative damage indexes, inflammatory factors, cell cycle, cell apoptosis, cell senescence, and their related proteins were analyzed by methyl thiazolyl tetrazolium (MTT) assay, enzyme-linked immunosorbent assay (ELISA), propidium iodide (PI) staining, annexin V-FITC/PI double staining, SA β-galactosidase staining, and western blotting (WB). The results showed that H_2O_2-induced cell growth inhibition rate decreased as supplementation with characteristic components when compared to H_2O_2 group. Meanwhile, the contents of antioxidant indexes (reactive oxygen species, lactate dehydrogenase, molondialdehyde, superoxide dismutase, glutathione), inflammatory factors (nuclear factor kappa-B, intercellular cell adhesion molecule-1, vascular cell adhesion protein 1), and functional factors (NO, Endothelin-1) in characteristic components treated groups improved if comparison with H_2O_2 group, suggesting the characteristic components of *E. ulmoides* could alleviate H_2O_2-induced oxidative damage. Moreover, cell cycle, cell apoptosis, cell senescence, and their related proteins under characteristic components treatment exhibited a better effect than under H_2O_2 treatment, implying the characteristic components could participate in anti-aging via multiple pathways. These results manifested that the characteristic components of *E. ulmoides* posses the capacity of anti-aging, which provided a basis for investigating the anti-aging ability of *E. ulmoides* itself.

KEYWORDS

Anti-aging; *Eucommia ulmoides*; characteristic components; oxidative damage; cell senescence

1 Introduction

Free radical theory of aging, is a popular suggested hallmarks of aging [1], implicates the gradual accumulation of oxidative cellular damage as a fundamental driver of cellular aging [2]. Plenty of factors

are responsible for free radical excessive production, such as genome instability, proteostasis failure, and environmental influence [3]. These factors can cause abnormal energy supply and metabolite production, which results in free oxygen radicals *in vivo* elevation. Reactive oxygen species (ROS) is one of the most important free oxygen radicals and can lead to numerous oxidative damages, such as carbonylation, oxidized methionine, glycation, aggregation of proteins, and DNA damage. Therefore, ROS extensively generation contributes to aging and age-related diseases (ARDs) occur, e.g., Alzheimer's disease, cancer, atherosclerosis, and metabolic diseases [4].

In recent years, the molecular mechanisms relevant to age-related progression through external natural products intervention have attracted much attention. For instance, natural products can modulate cellular longevity through histone post-translational modification and can induce the up-regulation of autophagy [5]. Meanwhile, kinds of natural products have been reported to slow anti-aging progress and can extend lifespan of organisms, such as resveratrol, astaxanthin, and gallic acid [6–8]. To date, more than 300 compounds or clinical drugs are announced with anti-aging activity. Among them, 185 compounds and 55 complex or extracts belong to natural products [3]. In addition, some of these compounds receive popular interest and present anti-aging activities in multiple aging models under vigorous investigation, such as chlorogenic acid from *Eucommia ulmoides* reveals anti-aging activity in *Caenorhabditis elegans* aging model [9].

Eucommia ulmoides Oliv. is the unique medicinal plant of China, and a total of 138 kinds of natural active compounds are separated, purified, and identified from the barks and leafs [10], such as chlorogenic acid, geniposidic acid, and aucubin. Based on the rich material foundation, *E. ulmoides* has multiple pharmacological activities, such as anti-inflammatory and anti-hyperlipidemia [11,12]. Chlorogenic acid (CA) is the most important characteristic component of *E. ulmoides*. It is reported that CA can protect mice against Cd-induced hepatorenal injury [13]. Moreover, research shows that the serum levels of Immunoglobulin A (Ig A), immunoglobulin G(Ig G), and immunoglobulin M (Ig M) increase under the function of *E. ulmoides* treatment, which contributes to immunity enhancement in animals [14]. Except CA, there are other characteristic components with high contents in *E. ulmoides*, e.g., geniposidic acid (GPA), aucubin (AU), and quercetin (QU). These components possess the abilities of free radical scavenging, anti-inflammatory, and anti anti-cancer [15–17]. However, although literatures about the four characteristic components reveal good to excellent biological functions, there is no systematic study about their effect on anti-aging, especially for GPA and AU.

In this study, the potential anti-aging activities of the four characteristic components from *E. ulmoides* were investigated. The antioxidant indexes, inflammatory factors, cell cycle, cell apoptosis, cell senescence, and their related proteins were analyzed. We hypothesis that the four characteristic components of *E. ulmoides* can alleviate H_2O_2-induced cell senescence based on their pharmacological activities. Our study will provide a theoretical foundation for evaluating the anti-aging ability of *E. ulmoides* itself, which contributes to the actually application of *E. ulmoides* in the field of functional foods and medicals.

2 Materials and Methods

2.1 Cell Material and Treatment

Human umbilical vein endothelial cell (HUVEC) was provided by Jiangsu KeyGEN BioTECH Co., Ltd., Nanjing, China, and incubated in F-12K medium (90%) with adding fetal bovine serum (FBS, 10%). The culture condition was under saturation humidity, 37°C, and 5% CO_2. The oxidative damage model of HUVEC was established by culturing 70% HUVEC *in vitro* containing 100 μM H_2O_2. Four major characteristic components of *E. ulmoides*, including chlorogenic acid (CA), geniposidic acid (GPA), aucubin (AU), and quercetin (QU), were adopted to access their potential anti-aging abilities. A negative control was prepared without adding H_2O_2 and characteristic components. Therefore, six groups were generated and divided into Control group, H_2O_2 group, H_2O_2 + CA group, H_2O_2 + GPA group,

H_2O_2 + AU group, and H_2O_2 + QU group. Meanwhile, the groups inclusion H_2O_2 were denoted as H_2O_2 treated groups. The HUVEC of each group was treated for 24 h and these treated cells were used for anti-aging evaluation unless otherwise specified.

2.2 Methyl Thiazolyl Tetrazolium (MTT) Cell Proliferation Assay

The cell suspension (100 μL) was added to each well (96-well plates) at a cell density of 5×10^4 /mL and incubated at 37°C, 5% CO_2 for 24 h. Meanwhile, medium alone (100 μL) was prepared as negative control and incubated at the same condition. After incubation, 5 mg/mL MTT solution (20 μL) was added to each well and incubated for another 4 h. When incubation completed, the medium of each well was subsequently removed. DMSO (150 μL) was added to each well and mixed thoroughly with the pipette. The optical density (OD) value of each well was recorded at 490 nm.

2.3 Intracellular ROS/Anti-Oxidation Indexes Detection

The intracellular ROS level was assayed with 2,7-dichlorodi-hydrofluorescein diacetate (DCFH-DA) fluorescent probe. The treated HUVEC of each group was washed with phosphate buffered saline (PBS) and collected at 1000 rpm for 5 min. The cell density was adjusted to 1×10^6 /mL. Then, the cells were resuspended in DCFH-DA and incubated at 37°C for 20 min with vibrating every five minutes. Loaded cells were washed three times by serum-free cell culture medium. The fluorescence intensity of each group was determined by using a fluorescence microscope with an excitation wavelength of 488 nm and emission wavelength of 530 nm. The intracellular anti-oxidation related indexes were determined by using relevant detection kit, including lactate dehydrogenase (LDH), malondialdehyde (MDA), superoxide dismutase (SOD), and glutathione (GSH) (Jiangsu KeyGEN BioTECH Co., Ltd., Nanjing, China). The pertinent details of detection was followed the instruction of each kit.

2.4 Functional and Inflammatory Factors Detection by Enzyme-Linked Immunosorbent Assay (ELISA)

Two functional factors (NO, ET-1) and three inflammatory factors (NF-κB, ICAM-1, VCAM-1) of the treated HUVEC from each group were determined by using relevant detection kits. The NO content was assayed by chemical method and the ET-1, NF-κB, ICAM-1, and VCAM-1 contents were monitored by ELISA. All of the kits were purchased from Jiangsu KeyGEN BioTECH Co., Ltd, Nanjing, China. The pertinent details of detection was followed the instruction of each kit.

2.5 Cell Cycle Detection by Propidium Iodide (PI) Staining

The most commonly used dye for cell cycle analysis was propidium iodide (PI) staining. After digested with 0.25% trypsin and washed twice with PBS, cells were harvested at a density of 5×10^5/mL. The prepared single cell suspension was fixed with 70% ethanol at 4°C for 2 h. Then, the cell suspension was mixed with a solution containing 100 μL RNase A (37°C, 30 min) and 400 μL PI, and incubated in the dark at 4°C for 30 min. The red fluorescence of each group was recorded at 488 nm.

2.6 Cell Apoptosis Detection by Annexin V-FITC/PI Double Staining

The cell apoptosis rate of the treated HUVEC from each group was determined by using annexin V-FITC/PI double staining detection kit (Jiangsu KeyGEN BioTECH Co., Ltd., Nanjing, China). After digested with 0.25% trypsin and washed twice with PBS, cells were harvested at a density of 5×10^5/mL. The prepared single cell suspension was mixed with 500 μL Binding Buffer, 5 μL Annexin V-FITC, and 5 μL PI completely. Then, the cell suspension was incubated in the dark for 15 min. The cell apoptosis rate was detected on a flow cytometer (FCM).

2.7 Cell Senescence Detection by SA β-galactosidase Staining

The treated HUVEC of each group was inoculated in a 6-well plate and washed with PBS. A working solution of *β*-galactosidase (1 mL) stain was then added, mixed well, and incubated at 37°C for 15 min. After incubation, the *β*-galactosidase stain solution was removed and washed with PBS for three times every three minutes. Then, the PBS was draw out and 1 mL *β*-galactosidase stain solution was added to each well. The senescence of cells in each group was observed under microscope.

2.8 Western Blotting (WB) Analysis

Ten inflammatory, apoptosis/senescence, and DNA-repair process related proteins were selected for western blotting (WB) analysis. The detail information of the ten proteins is shown in Table S1. The total protein of the treated HUVEC from each group was isolated by using Whole Cell Lysis Assay kit (Jiangsu KeyGEN BioTECH Co., Ltd., Nanjing, China). Protein quantitation for the isolated whole protein was carried out by using BCA Protein Quantitation Assay kit (Jiangsu KeyGEN BioTECH Co., Ltd., Nanjing, China). Then, the total protein (30 μg) of each group was separated by sodium dodecyl sulfate polyacrylamide gel electrophoresis (SDS-PAGE), which was prepared by SDS-PAGE Prepare kit (Jiangsu KeyGEN BioTECH Co., Ltd., Nanjing, China). The band of target protein was transferred to a nitrocellulose (NC) membrane at 200 mA for 2 h and subsequently sealed in 5% nonfat-dried milk for another 2 h. Then, the NC membrane was saturated in a plate inclusion primary antibody at 4°C overnight. The next day, the NC membrane was washed three times (10 min/time) with Tris Buffered Saline Tween (TBST) and saturated in a 5% nonfat-dried milk inclusion secondary antibody (Goat Anti-Rabbit Ig G-HRP) for 2 h. After incubation, NC membrane was washed three times (10 min/time) with TBST and detected by electrochemiluminescence (ECL). The imaging of selected proteins were photographed by BOX Chemi XR5 (SYNGENE, Cambridge, United Kingdom) and the relative expression of target protein was analyzed by Gel-Pro32 software.

2.9 Statistical Analysis

All data were analyzed by using Microsoft Office and SPSS 19.0, and were expressed as the mean ± SD. One-way analysis of variance (ANOVA) and the least significant difference (LSD) tests were performed to identify significant differences among the tested groups. Tukey test was used to correct multiple comparisons.

3 Results and Discussions

3.1 Inhibition Rate of HUVEC

The inhibition rates of the four characteristic components against HUVEC are shown in Fig. 1A. At the threshold of inhibition rate < 10%, the selected optimum concentrations of CA, GPA, AU, and QU were 0.78, 3.13, 50.00, and 6.13 μM, respectively. Meanwhile, the inhibition rate of H_2O_2 against HUVEC was greater than 50% (Fig. 1B), suggesting the HUVEC under 100 μM H_2O_2 treatment was the desirable oxidative damage model for anti-aging analysis. Significant decrease in inhibition rate was observed when H_2O_2 supplementation with characteristic component treatment ($p < 0.05$, Fig. 1B). However, the inhibition rates of HUVEC revealed no significant difference among the four characteristic components added groups ($p > 0.05$).

3.2 Contents of ROS/ROS-Related Indexes

Cell injury is tightly related to oxidative stress, which induces amount of ROS generation and cause oxidative damage as well as cell dysfunction [18]. As a strong oxidant, H_2O_2 can induce lipid peroxidation and promote ROS production [19]. In our study, the ROS contents in all H_2O_2 treated groups were higher than that of in control group (Fig. 2, Fig. S1). Compared to H_2O_2 group, the characteristic component added groups revealed lower ROS contents, especially in GPA and AU added groups, indicating the characteristic components of *E. ulmoides* could reduce the H_2O_2-induced oxidative damage.

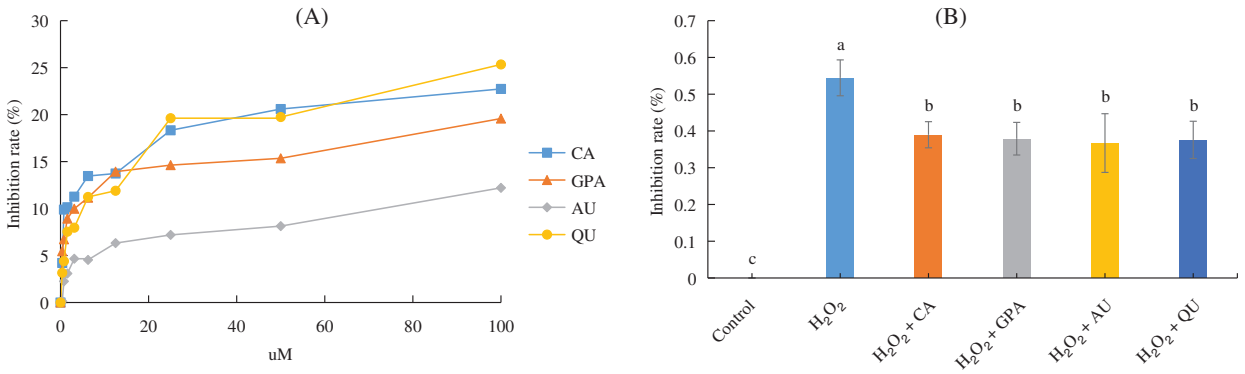

Figure 1: The inhibition rate (%) of HUVEC. (A) Inhibition rate of HUVEC under four characteristic components treatment; (B) Inhibition rate of HUVEC of the six tested groups. CA, GPA, AU, and QU represent chlorogenic acid, geniposidic acid, aucubin, and quercetin, respectively

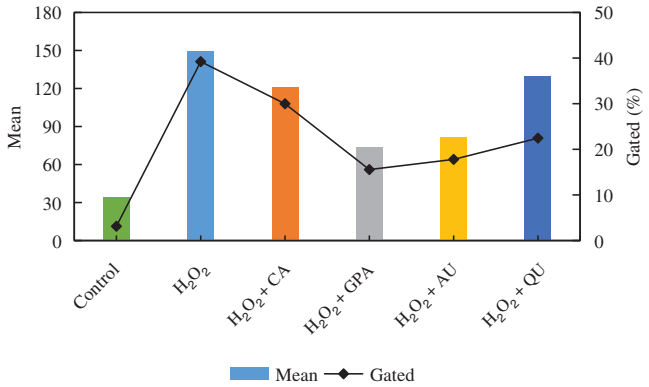

Figure 2: The intracellular ROS content among the six tested groups. CA, GPA, AU, and QU represent chlorogenic acid, geniposidic acid, aucubin, and quercetin, respectively

It is reported that LDH activity and MDA content can reflect the effect of H_2O_2 on cell membrane integrity and the degree of lipid peroxidation [20]. Besides, intracellular SOD activity and GSH content can positively take part in cell damage response via scavenging free radical [21]. Hence, these four ROS-related indexes are explored. The MDA exhibited the similar profile with ROS and its content was significantly higher in H_2O_2 group, followed by CA, AU, and QU added groups, and was significantly lower in control and GPA added group ($p < 0.05$, Table 1). The GSH content and SOD activity in GPA and AU added groups were significantly higher than in other H_2O_2 treated groups, but were significantly lower than in control group ($p < 0.05$, Table 1). On the contrary, the energy-related LDH activity in GPA and AU added groups were significantly lower than that of in other H_2O_2 treated groups, but were significantly higher than that of in control group ($p < 0.05$, Table 1). According to these results, it was easily to summary that the characteristic components of *E. ulmoides* could enhance the antioxidant ability of cells and had advantages in maintaining cell function as normal, especially in GPA and AU added groups.

3.3 Contents of Functional and Inflammatory Factors

Because the H_2O_2-induced oxidative damages inevitably occur, the consequent inflammatory response in HUVEC is therefore explored. Three typical inflammatory factors were investigated in our study, including NF-κB, ICAM-1, and VCAM-1 (Table 2). The contents of NF-κB, ICAM-1, and VCAM-1

increased in H_2O_2 group and significantly decreased in characteristic components added groups ($p < 0.05$). Apart from the effect of QU on ICAM-1, the overall effects of supplementation with GPA and AU on NF-κB, ICAM-1, and VCAM-1 contents were better than CA and QU. Previous researches have indicated the three inflammatory factors are well associated with HUVEC inflammation and can promote the migration and adhesion of white blood cell (WBC) to HUVEC [22]. Among these factors, NF-κB dominates the key position as its activation is ROS-dependent [23] and many ARDs are coordinated by increasing NF-κB levels [24]. For instance, ICAM-1 and VCAM-1 are tightly involvement with NF-κB based on their expressions are regulated by NF-κB activation in HUVEC [25]. Thus, our results revealed that the characteristic components of *E. ulmoides* could alleviate H_2O_2-induced inflammation.

Table 1: The intracellular anti-oxidation indexes contents among the six tested groups

Group	Control	H_2O_2	H_2O_2 + CA	H_2O_2 + GPA	H_2O_2 + AU	H_2O_2 + QU
LDH (U/L)	22.66 ± 1.00 e	58.39 ± 1.00 a	39.43 ± 1.64 c	33.77 ± 1.00 d	32.03 ± 1.31 d	45.32 ± 1.00 b
MDA (nmol)	7.42 ± 0.42 c	24.96 ± 1.70 a	13.33 ± 0.45 b	8.32 ± 0.30 c	13.96 ± 0.48 b	13.70 ± 0.36 b
GSH (gGSH/L)	437.94 ± 9.11 a	154.22 ± 8.70 e	271.24 ± 27.87 c	376.05 ± 7.15 b	378.13 ± 1.96 b	236.65 ± 17.45 d
SOD (U/ml)	59.95 ± 0.70 a	25.89 ± 2.24 d	27.76 ± 2.58 cd	39.62 ± 1.46 b	36.59 ± 1.28 b	29.56 ± 1.40 c

Note: CA, GPA, AU, and QU represent chlorogenic acid, geniposidic acid, aucubin, and quercetin, respectively.

Table 2: The functional and inflammatory factors contents among the six tested groups

Group	Control	H_2O_2	H_2O_2 + CA	H_2O_2 + GPA	H_2O_2 + AU	H_2O_2 + QU
NO (uM/L)	32.37 ± 1.99 a	14.47 ± 1.83 d	16.56 ± 0.45 cd	24.80 ± 2.02 b	19.45 ± 2.07 c	27.81 ± 1.24 b
ET-1 (pg/mL)	182.00 ± 7.59 c	254.95 ± 12.38 a	220.44 ± 6.77 b	223.61 ± 6.78 b	221.15 ± 5.90 b	214.88 ± 7.90 b
NF-κB (ng/ml)	10.21 ± 1.61 d	35.17 ± 2.67 a	20.30 ± 2.22 bc	21.39 ± 1.93 bc	19.49 ± 0.64 c	23.62 ± 1.52 b
ICAM-1 (ng/ml)	8.44 ± 0.55 e	26.51 ± 1.09 a	14.62 ± 0.75 b	12.68 ± 0.81 c	13.82 ± 0.83 bc	11.03 ± 0.93 d
VCAM-1 (pg/ml)	163.52 ± 13.78 d	342.46 ± 12.44 a	307.33 ± 9.54 b	282.79 ± 8.55 c	265.23 ± 14.08 c	314.25 ± 15.53 b

Note: CA, GPA, AU, and QU represent chlorogenic acid, geniposidic acid, aucubin, and quercetin, respectively.

Together with the inflammatory factors, the proteins related to NF-κB activation were also analyzed, including p65, P-Rb, and P-ERK (Table 3, Fig. 3, Table S2). Functioned as the subunit of NF-κB, p65 comprises a powerful transcriptional activation domain [26]. Simultaneously, P-Rb and P-ERK positively participate in regulation the expression of NF-κB activation [27,28]. Interestingly, no significant difference was observed for the expressions of p65 among H_2O_2 treated groups ($p > 0.05$). However, the relative expressions of P-Rb and P-ERK were induced significantly up-regulation under H_2O_2 treatment ($p < 0.05$) and would decrease as supplementation with characteristic components, especially in GPA and AU added groups. Based on above-mentioned points, we thus speculated that the characteristic components of *E. ulmoides* contributed to inflammation remission.

Except the inflammatory factors, the HUVEC secretion related vascular active factors are studied in tandem, including NO and ET-1, which participate in physiological and pathological reactions of vasoconstriction and vasodilatation [29]. As shown in Table 2, NO content significantly decreased in H_2O_2 group, whereas the content increased in characteristic components added groups, especially in GPA and QU added groups ($p < 0.05$), which was in accordance with *E. ulmoides* extract could activate NO production in Dahl salt sensitive rats [30]. Opposite of NO content, up-regulation of ET-1 content was observed in H_2O_2 group and the content would significantly decrease as supplementation with characteristic components ($p < 0.05$). Consequently, we obtained that the characteristic components of *E. ulmoides* could reduce H_2O_2-induced inflammation and keep the normal cellular function of HUVEC.

Table 3: The relative expression of inflammatory, apoptosis/senescence, and DNA-repair process related proteins among the six tested groups

Group		Control	H_2O_2	H_2O_2 + CA	H_2O_2 + GPA	H_2O_2 + AU	H_2O_2 + QU
DNA-repair process	p16	0.06 ± 0.01 d	0.61 ± 0.03 a	0.41 ± 0.02 b	0.35 ± 0.04 c	0.33 ± 0.03 c	0.44 ± 0.03 b
	p21	0.14 ± 0.03 c	0.42 ± 0.04 a	0.39 ± 0.06 a	0.25 ± 0.04 b	0.24 ± 0.06 b	0.36 ± 0.03 a
	p53	0.04 ± 0.01 e	0.28 ± 0.02 a	0.16 ± 0.01 c	0.11 ± 0.01 d	0.12 ± 0.01 d	0.20 ± 0.01 b
Inflammatory	p65	0.05 ± 0.01 b	0.22 ± 0.02 a	0.24 ± 0.02 a	0.25 ± 0.02 a	0.25 ± 0.04 a	0.24 ± 0.02 a
	P-Rb	0.06 ± 0.01 d	0.25 ± 0.02 a	0.16 ± 0.02 b	0.11 ± 0.01 c	0.12 ± 0.01 c	0.18 ± 0.02 b
	P-ERK	0.45 ± 0.02 c	0.75 ± 0.04 a	0.71 ± 0.05 a	0.59 ± 0.01 b	0.60 ± 0.02 b	0.55 ± 0.05 b
Apoptosis/ Senescence	Bax	0.08 ± 0.01 c	0.28 ± 0.02 a	0.29 ± 0.02 a	0.23 ± 0.01 b	0.28 ± 0.02 a	0.28 ± 0.02 a
	Sirt1	0.20 ± 0.01 a	0.02 ± 0.01 d	0.04 ± 0.01 c	0.07 ± 0.01 b	0.05 ± 0.01 c	0.04 ± 0.01 c
	Bcl-2	0.10 ± 0.01 a	0.02 ± 0.002 cd	0.04 ± 0.01 bc	0.04 ± 0.003 b	0.04 ± 0.002 b	0.02 ± 0.01 d
	Survivin	0.26 ± 0.02 a	0.14 ± 0.01 bc	0.16 ± 0.02 b	0.14 ± 0.01 bc	0.14 ± 0.02 bc	0.11 ± 0.01 c

Note: CA, GPA, AU, and QU represent chlorogenic acid, geniposidic acid, aucubin, and quercetin, respectively.

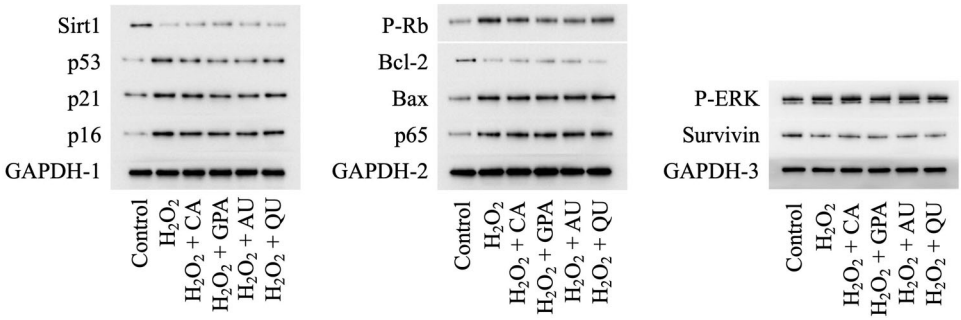

Figure 3: Effects of H_2O_2 and characteristic components on the expression levels of selected proteins. CA, GPA, AU, and QU represent chlorogenic acid, geniposidic acid, aucubin, and quercetin, respectively

3.4 Cell Cycle

Previous research has certified that H_2O_2-induced DNA-damage can lead to cell cycle arrest [31]. Since natural active components possess the ability of radical scavenging, these components reveal excellent protective effects against H_2O_2-induced DNA-damage, such as phenolics oleuropein and hydroxytyrosol from olive oil [32]. In this study, the cell cycle under H_2O_2 as well as under characteristic component treatments was determined (Fig. 4, Fig. S2). The proportion of G1 phase in H_2O_2 group was higher than that of in control group, accompanied with lower proportion of S phase, indicating that HUVEC got arrested in the G1 phase under H_2O_2 treatment. Although the proportion of G1 phase in characteristic components added groups decreased to the same level with control group, the proportion of S phase revealed obviously difference. Compared to control group, the proportion of S phase was higher in GPA and AU added groups, but was lower in CA and QU added groups, implying GPA and AU could facilitate HUVEC progress through to the S phase (stage of DNA synthesis) to avoid the H_2O_2-induced DNA-damage. DNA-damage response (DDR) is responsible for the coordination of DNA-damage cell cycle–checkpoint activation with DNA-repair processes. The DDR is a kinase-based signaling network that controls various effector proteins to achieve the coordination of the DNA-repair process, including p16, p21, and p53 [33]. Hence, the relative expressions of p16, p21, and p53 were investigated (Table 3). The expressions of p16, p21, and p53 significantly increased in H_2O_2 group and significantly decreased as supplementation with characteristic components ($p < 0.05$), especially in GPA and AU added groups.

Therefore, it could infer that the characteristic components of *E. ulmoides* positively participated in the DNA-repair processes and ensued DNA synthesis as normal.

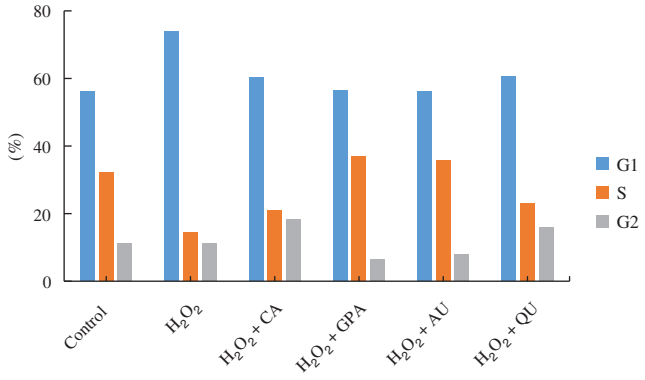

Figure 4: The cell cycle of HUVEC among the six tested groups. CA, GPA, AU, and QU represent chlorogenic acid, geniposidic acid, aucubin, and quercetin, respectively

3.5 Cell Apoptosis Rate

Accompany with cell cycle arrest under H_2O_2 treatment, the cell apoptosis rate will increase [31]. In the present study, the cell apoptosis rate in control group was 6.49% and was apparently lower than that of in H_2O_2 group (40.66%) (Table 4, Fig. S3), indicating that H_2O_2 treatment caused oxidative damage. A slightly reduction in cell apoptosis rate was observed in characteristic component added groups. Among the four characteristic components added groups, GPA added group revealed the best result and its apoptosis rate decreased to 36.64%, followed by CA (37.94%) and AU (37.99%) added groups, and was higher in QU added group (38.94%). Meanwhile, GPA and AU mainly reduced the early apoptosis of HUVEC and their apoptosis rates were 26.09% and 27.51%, respectively, which were lower than in CA (30.90%) and QU (30.07%) added groups. Cell apoptosis is closely related to cell senescence in DNA-damaged cells and there are kinds of proteins function in DDR-associated pathways, such as Sirt1, Bcl-2, Survivin, and Bax. Former study has indicated that Sirt1 is necessary for p53 deacetylation and its loss promotes cell apoptosis [34]. Meanwhile, Bcl-2 acts as anti-apoptotic factors in the mitochondria apoptotic signaling pathways, whereas Bax acts as an pro-apoptotic factor. These two factors can regulate apoptosis via controlling mitochondrial membrane permeability to release apoptosis activators [35,36]. Moreover, Survivin is an inhibitor of apoptosis (IAP) family protein, which is involved in various protein-protein interactions (PPIs) and thereby regulates cell apoptosis [37]. Therefore, Sirt1, Bcl-2, and Survivin take function in anti-apoptosis, whereas Bax takes function in pro-apoptosis. Accordance with the profile of apoptosis rate alteration, the relative expressions of Sirt1, Bcl-2, and Survivin significantly decreased under H_2O_2 treatment, but the decreasing amplitude would be suppressed as characteristic components supplemented (Table 3). Besides, the relative expression of Bax would be induced significant up-regulation under H_2O_2 treatment and its expression in GPA added group significantly decreased ($p < 0.05$). These results suggested that the characteristic components of *E. ulmoides* could inhibit cell apoptosis.

3.6 SA β-gal Staining

Apart from the results of cell cycle and cell apoptosis, the senescence-associated SA-β-gal activity analysis is conducted to reflect the senescent cells in culture [38]. Compared to control group, the SA β-gal stained positive cells increased in all H_2O_2 treated groups with squamous cell emerging (Fig. 5), suggesting that H_2O_2 treatment accelerated cell senescence. However, the SA β-gal stained positive cells in characteristic components added groups were lower than that of in H_2O_2 group, indicating the

characteristic components of *E. ulmoides* possessed the ability of protecting cells and could alleviate the H_2O_2-induced cell aging. Consistent with former results, the GPA added group revealed the least stained positive cells among the four characteristic components added groups, followed by AU added group. Moreover, at the threshold of cell inhibition rate < 10%, the optimum concentration of the four characteristic components ranked as CA (0.781 μM) < GPA (3.125 μM) < QU (6.125 μM) < AU (50 μM). Therefore, the dosage of GPA was kept at a relative low level. Combine the above-mentioned points together, it could get that GPA had a great promise in anti-aging research.

Table 4: The cell apoptosis rate among the six tested groups

Group	UL (%)	UR (%)	LL (%)	LR (%)	Apoptosis (%)
Control	2.06	2.38	91.45	4.11	6.49
H_2O_2	2.79	7.77	56.55	32.89	40.66
H_2O_2 + CA	2.97	7.04	59.09	30.90	37.94
H_2O_2 + GPA	3.31	10.55	60.04	26.09	36.64
H_2O_2 + AU	3.12	10.48	58.90	27.51	37.99
H_2O_2 + QU	3.10	8.87	57.97	30.07	38.94

Notes: CA, GPA, AU, and QU represent chlorogenic acid, geniposidic acid, aucubin, and quercetin, respectively. UL, UR, LL, and LR represent upper left, upper right, lower left, and lower right quadrant in the spectrum of Annexin V-FITC/PI double staining, respectively.

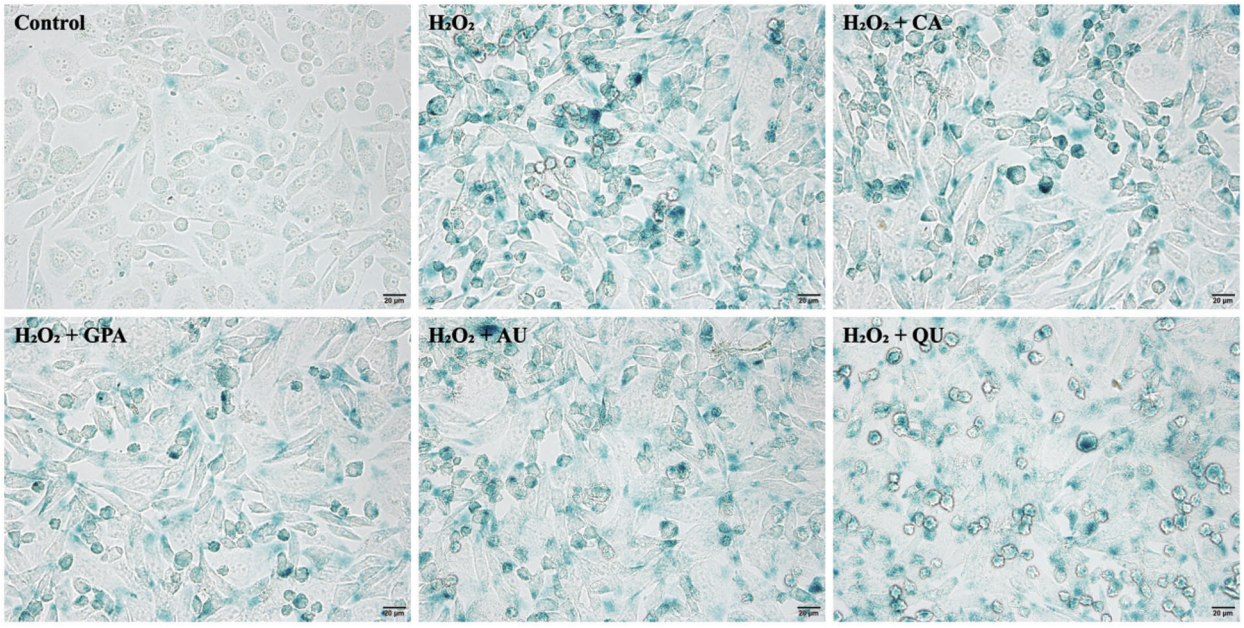

Figure 5: The SA *β*-gal staining of HUVEC among the six tested groups. CA, GPA, AU, and QU represent chlorogenic acid, geniposidic acid, aucubin, and quercetin, respectively

4 Conclusion

Comprehensive the above-mentioned points, it can conclude that the four characteristic components of *E. ulmoides* reveal the ability of facilitating DNA synthesis, inhibiting cell apoptosis, and alleviating cell

senescence, and these results may further certify *E. ulmoides* possess the ability of anti-aging. The conclusions from the preliminary data and discussion can be summarized as follows:

1. The H_2O_2-induced cell growth inhibition rate as well as the contents of ROS related antioxidant indexes (LDH, MDA, SOD, GSH) improve as supplementation with characteristic components, indicating the four characteristic components of *E. ulmoides* can alleviate H_2O_2-induced oxidative damage.
2. Typical inflammatory factors (NF-κB, ICAM-1, VCAM-1) and functional factors (NO, ET-1) are investigated to reflect the impacts of characteristic components on cells. The four selected characteristic components of *E. ulmoides* contribute to inflammation remission and have advantages in maintaining cellular function as normal.
3. The cell cycle, cell apoptosis, and cell senescence of H_2O_2-treated HUVEC ameliorate under characteristic components treatment. Meanwhile, DNA biosynthesis processes are activated by characteristic components, suggesting the characteristic components of *E. ulmoides* facilitate cell division to slow the aging process.
4. Among the four characteristic components, GPA reveals the most potential capacity in anti-aging, followed by AU. These two compounds of *E. ulmoides* possess tremendous application foreground in drug field and provide a scientific basis for *E. ulmoides* itself serving as a anti-aging material.

Funding Statement: This study was supported by the National Natural Science Foundation of China (Grant No. 42107020) and the Science and Technology Project of Hunan Province (2020SK2028).

Conflicts of Interest: The authors declare that they have no conflicts of interest to report regarding the present study.

References

1. López-Otín, C., Galluzzi, L., Freije, J. M., Madeo, F., Kroemer, G. (2016). Metabolic control of longevity. *Cell, 166(4),* 802–821. DOI 10.1016/j.cell.2016.07.031.
2. Harman, D. (1956). Aging: A theory based on free radical and radiation chemistry. *Journal of Gerontology, 11(3),* 298–300. DOI 10.1093/geronj/11.3.298.
3. Ding, A. J., Zheng, S. Q., Huang, X. B., Xing, T. K., Wu, G. S. et al. (2017). Current perspective in the discovery of anti-aging agents from natural products. *Natural Products and Bioprospecting, 7(5),* 335–404. DOI 10.1007/s13659-017-0135-9.
4. Ziada, A. S., Smith, M. S. R., Côté, H. C. F. (2020). Updating the free radical theory of aging. *Frontiers in Cell and Developmental Biology, 8,* 575645. DOI 10.3389/fcell.2020.575645.
5. Cătană, C. S., Atanasov, A. G., Berindan-Neagoe, I. (2018). Natural products with anti-aging potential: Affected targets and molecular mechanisms. *Biotechnology Advances, 36(6),* 1649–1656. DOI 10.1016/j.biotechadv.2018.03.012.
6. Saul, N., Pietsch, K., Sturzenbaum, S. R., Menzel, R., Steinberg, C. E. (2011). Diversity of polyphenol action in *Caenorhabditis elegans*: Between toxicity and longevity. *Journal of Natural Products, 74(8),* 1713–1720. DOI 10.1021/np200011a.
7. Wood, J. G., Rogina, B., Lavu, S., Howitz, K., Helfand, S. L. et al. (2004). Sirtuin activators mimic caloric restriction and delay ageing in metazoans. *Nature, 430(7000),* 686–689. DOI 10.1038/nature02789.
8. Yazaki, K., Yoshikoshi, C., Oshiro, S., Yanase, S. (2011). Supplemental cellular protection by a carotenoid extends lifespan via Ins/IGF-1 signaling in *Caenorhabditis elegans*. *Oxidative Medicine and Cellular Longevity, 2011,* 596240. DOI 10.1155/2011/596240.
9. Zheng, S. Q., Huang, X. B., Xing, T. K., Ding, A. J., Wu, G. S. et al. (2017). Chlorogenic acid extends the lifespan of *Caenorhabditis elegans* via insulin/IGF-1 signaling pathway. *Journals of Gerontology. Series A, Biological Sciences and Medical Sciences, 72(4),* 464–472. DOI 10.1093/gerona/glw105.

10. Wang, Z., Peng, S., Peng, M., She, Z., Yang, Q. et al. (2020). Adsorption and desorption characteristics of polyphenols from *Eucommia ulmoides* Oliv. leaves with macroporous resin and its inhibitory effect on α-amylase and α-glucosidase. *Annals of Translational Medicine, 8(16),* 1004. DOI 10.21037/atm-20-5468.
11. Gu, T., Li, G., Wu, X., Zeng, T., Xu, Q. et al. (2020). Effects of immunopotentiators on biochemical parameters, proinflammatory cytokine, and nonspecific immune responses in Shaoxing ducklings. *Poultry Science, 99(11),* 5461–5471. DOI 10.1016/j.psj.2020.08.069.
12. Wang, C. Y., Tang, L., He, J. W., Li, J., Wang, Y. Z. (2019). Ethnobotany, phytochemistry and pharmacological properties of *Eucommia ulmoides*: A review. *American Journal of Chinese Medicine, 47(2),* 259–300. DOI 10.1142/S0192415X19500137.
13. Ding, Y., Li, X., Liu, Y., Wang, S., Cheng, D. (2021). Protection mechanisms underlying oral administration of chlorogenic acid against cadmium-induced hepatorenal injury related to regulating intestinal flora balance. *Journal of Agricultural and Food Chemistry, 69(5),* 1675–1683. DOI 10.1021/acs.jafc.0c06698.
14. Abaidullah, M., Peng, S., Song, X., Zou, Y., Li, L. et al. (2021). Chlorogenic acid is a positive regulator of MDA5, TLR7 and NF-κB signaling pathways mediated antiviral responses against Gammacoronavirus infection. *International Immunopharmacology, 7(2),* 107671. DOI 10.1016/j.intimp.2021.107671.
15. Jaisankar, A. I., Arivarasu, L., Rajeshkumar, S. (2017). Free radical scavenging and anti-inflammatory activity of chlorogenic acid mediated silver nanoparticle. *Natural Products and Bioprospecting, 7,* 335–404. DOI 10.9734/jpri/2020/v32i1930715.
16. Háznagy-Radnai, E., Wéber, E., Czigle, S., Berkecz, R., Csedo, K. et al. (2014). Identification of Iridoids, flavonoids and triterpenes from the methanolic extract of *Melampyrum bihariense* A. Kern. and the antioxidant activity of the extract. *Chromatographia, 77,* 1153–1159. DOI 10.1007/s10337-014-2672-2.
17. Kim, S. H., Lee, J. C. (2021). Quercetin protects hepatocytes against CCl4-induced apoptosis via SIRT1 regulation. *Cell and Tissue Biology, 15(4),* 381–387. DOI 10.1134/S1990519X21040039.
18. Zachariah, M., Maamoun, H., Milano, L., Rayman, M. P., Meira, L. B. et al. (2021). Endoplasmic reticulum stress and oxidative stress drive endothelial dysfunction induced by high selenium. *Journal of Cellular Physiology, 236(6),* 4348–4359. DOI 10.1002/jcp.30175.
19. Hulsmans, M., Van Dooren, E., Holvoet, P. (2012). Mitochondrial reactive oxygen species and risk of atherosclerosis. *Current Atherosclerosis Reports, 14(3),* 264–276. DOI 10.1007/s11883-012-0237-0.
20. Ntaios, G., Gatselis, N. K., Makaritsis, K., Dalekos, G. N. (2013). Adipokines as mediators of endothelial function and atherosclerosis. *Atherosclerosis, 227(2),* 216–221. DOI 10.1016/j.atherosclerosis.2012.12.029.
21. Hu, M. C., Shi, M., Zhang, J., Quiñones, H., Griffith, C. et al. (2011). Klotho deficiency causes vascular calcification in chronic kidney disease. *Journal of the American Society of Nephrology, 22(1),* 124–136. DOI 10.1681/ASN.2009121311.
22. Devaraj, S., Syed, B., Chien, A., Jialal, I. (2012). Validation of an immunoassay for soluble Klotho protein decreased levels in diabetes and increased levels in chronic kidney disease. *The American Journal of Clinical Pathology, 137(3),* 479–485. DOI 10.1309/AJCPGPMAF7SFRBO4.
23. Simard, J. C., Cesaro, A., Chapeton-Montes, J., Tardif, M., Antoine, F. et al. (2013). S100A8 and S100A9 induce cytokine expression and regulate the NLRP3 inflammasome via ROS-dependent activation of NF-κB. *PLoS One, 8(8),* e72138. DOI 10.1371/journal.pone.0072138.
24. Cătană, C. S., Berindan-Neagoe, I. (2012). Aging and immunity. In: *Aging: The science of aging-general concepts*, pp. 6–10. Germany: Lambert Academic Publishing.
25. Kim, S. R., Bae, Y. H., Bae, S. K., Choi, K. S., Yoon, K. H. et al. (2008). Visfatin enhances ICAM-1 and VCAM-1 expression through ROS-dependent NF-κB activation in endothelial cells. *Biochimica et Biophysica Acta, 1783(5),* 886–895. DOI 10.1016/j.bbamcr.2008.01.004.
26. Vermeulen, L., Wilde, G. D., Damme, P. V., Berghe, W. V., Haegeman, G. (2003). Transcriptional activation of the NF-κB p65 subunit by mitogen- and stress-activated protein kinase-1 (MSK1). *EMBO Journal, 22(6),* 1313–1324. DOI 10.1093/emboj/cdg139.
27. Sundar, V., Tamizhselvi, R. (2020). Inhibition of Rb phosphorylation leads to H2S-mediated inhibition of NF-κB in acute pancreatitis and associated lung injury in mice. *Pancreatology, 20(4),* 647–658. DOI 10.1016/j.pan.2020.04.011.

28. Lv, Y., Zhang, Z., Hou, L., Zhang, L., Zhang, J. et al. (2015). Phytic acid attenuates inflammatory responses and the levels of NF-κB and p-ERK in MPTP-induced Parkinson's disease model of mice. *Neuroscience Letters, 597,* 132–136. DOI 10.1016/j.neulet.2015.04.040.
29. Kurosu, H., Yamamoto, M., Clark, J. D., Pastor, J. V., Nandi, A. et al. (2005). Suppression of aging in mice by the hormone Klotho. *Science, 309(5742),* 1829–1833. DOI 10.1126/science.1112766.
30. Ishimitsu, A., Tojo, A., Satonaka, H., Ishimitsu, T. (2021). *Eucommia ulmoides* (Tochu) and its extract geniposidic acid reduced blood pressure and improved renal hemodynamics. *Biomedicine & Pharmacotherapy, 141,* 111901. DOI 10.1016/j.biopha.2021.111901.
31. Manoel-Caetano, F. S., Rossi, A. F. T., Ribeiro, M. L., Prates, J., Oliani, S. M. et al. (2020). Hydrogen peroxide and Helicobacter pylori extract treatment combined with APE1 knockdown induce DNA damage, G2/M arrest and cell death in gastric cancer cell line. *DNA Repair, 96,* 102976. DOI 10.1016/j.dnarep.2020.102976.
32. Zorić, N., Kopjar, N., Rodriguez, J. V., Tomić, S., Kosalec, I. (2021). Protective effects of olive oil phenolics oleuropein and hydroxytyrosol against hydrogen peroxide-induced DNA damage in human peripheral lymphocytes. *Acta Pharmaceutica, 71(1),* 131–141. DOI 10.2478/acph-2021-0003.
33. Kulaberoglu, Y., Gundogdu, R., Hergovich, A. (2016). The role of p53/p21/p16 in DNA-damage signaling and DNA repair. *Genome Stability, 13(7),* 243–256. DOI 10.1016/B978-0-12-803309-8.00015-X.
34. Bartoli-Leonard, F., Wilkinson, F. L., Schiro, A., Inglott, F. S., Alexander, M. Y. et al. (2021). Loss of SIRT1 in diabetes accelerates DNA damage-induced vascular calcification. *Cardiovascular Research, 117(3),* 836–849. DOI 10.1093/cvr/cvaa134.
35. Hu, L. G., Sun, Y. K., Hu, J. (2010). Catalpol inhibits apoptosis in hydrogen peroxide-induced endothelium by activating the PI3K/ AKT signaling pathway and modulating expression of Bcl-2 and Bax. *European Journal of Pharmacology, 628(1–3),* 155–163. DOI 10.1016/j.ejphar.2009.11.046.
36. Ling, Y., Lu, N., Gao, Y., Chen, Y., Wang, S. et al. (2009). Endostar induces apoptotic effects in HUVECs through activation of caspase-3 and decrease of Bcl-2. *Anticancer Research, 29(1),* 411–417.
37. Sarvagalla, S., Lin, T. Y., Kondapuram, S. K., Cheung, C. H. A., Coumar, M. S. (2021). Survivin-caspase protein-protein interaction: Experimental evidence and computational investigations to decipher the hotspot residues for drug targeting. *Journal of Molecular Structure, 1229(4),* 129619. DOI 10.1016/j.molstruc.2020.129619.
38. Debacq-Chainiaux, F., Erusalimsky, J. D., Campisi, J., Toussaint, O. (2009). Protocols to detect senescence-associated beta-galactosidase (SA-betagal) activity, a biomarker of senescent cells in culture and in vivo. *Nature Protocols, 4(12),* 1798–1806. DOI 10.1038/nprot.2009.191.

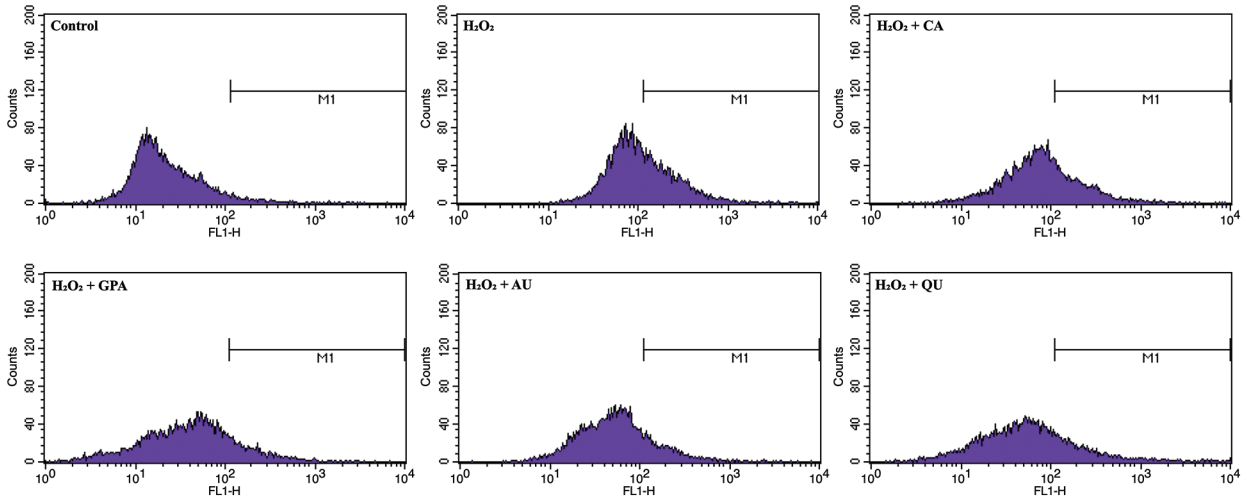

Figure S1: The spectrum of intracellular ROS content among the six tested groups. CA, GPA, AU, and QU represent chlorogenic acid, geniposidic acid, aucubin, and quercetin, respectively

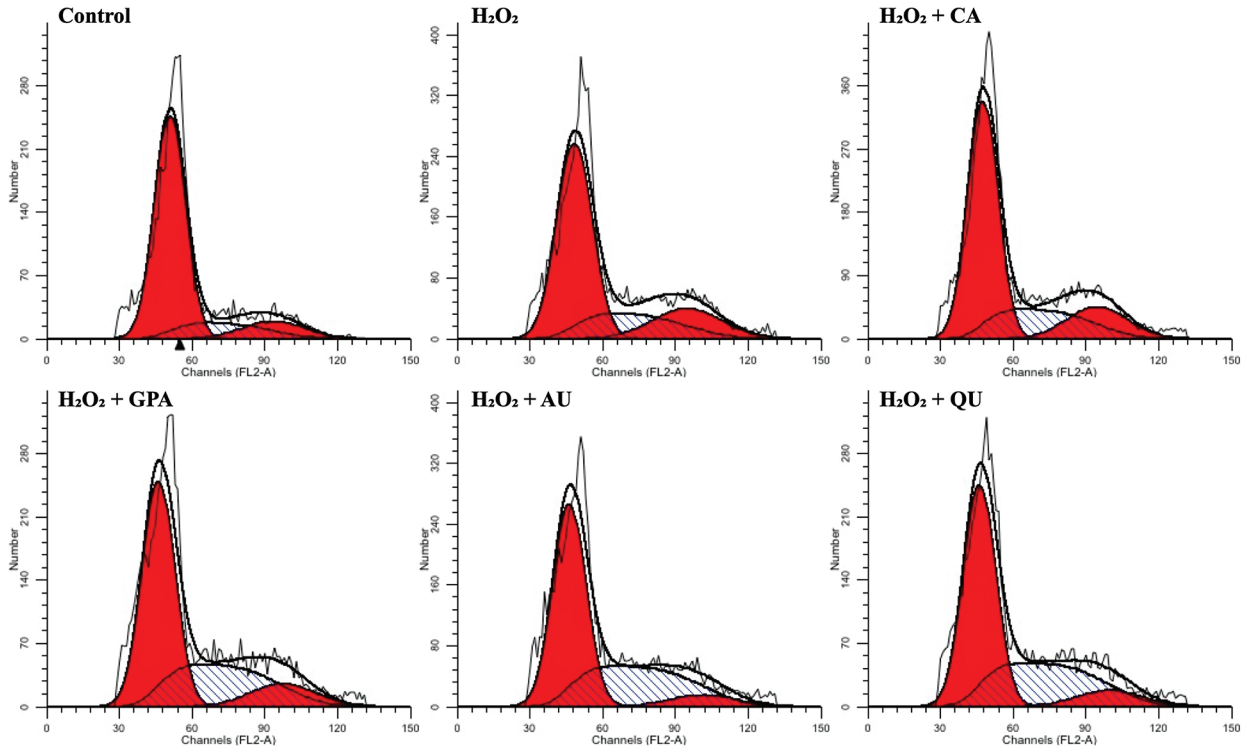

Figure S2: The spectrum of PI staining among the six tested groups. CA, GPA, AU, and QU represent chlorogenic acid, geniposidic acid, aucubin, and quercetin, respectively

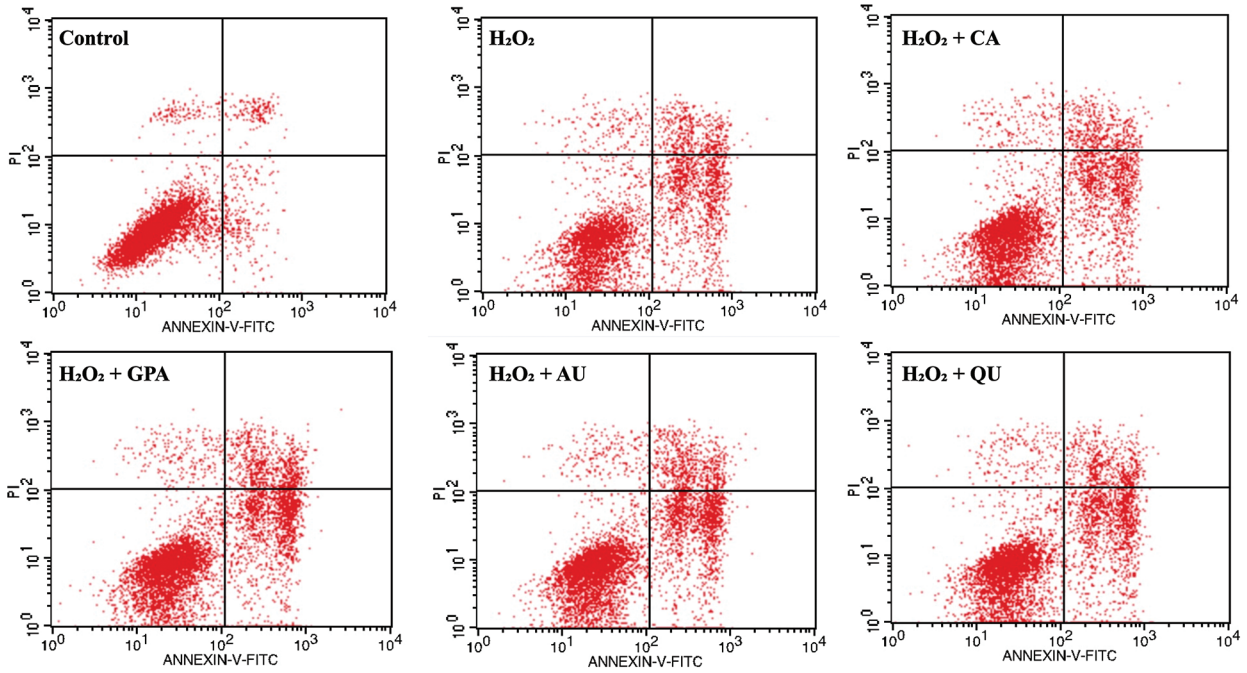

Figure S3: The spectrum of Annexin V-FITC/PI double staining among the six tested groups. CA, GPA, AU, and QU represent chlorogenic acid, geniposidic acid, aucubin, and quercetin, respectively

Table S1: The detail information of the ten selected proteins for western blotting (WB) analysis

Protein	Molecular weight (kDa)	Dilution rate	Gel concentration for SDS-PAGE
p16	16	1:1000	12%
p21	21	1:1000	12%
p53	53	1:200	10%
p65	65	1:1000	10%
P-Rb	106	1:1000	10%
P-ERK	44	1:1000	10%
Bax	21	1:1000	12%
Sirt1	110	1:20000	10%
Bcl-2	26	1:1000	12%
Survivin	16	1:5000	12%

Table S2: The fluorescence value of inflammatory, apoptosis/senescence, and DNA-repair process related proteins among the six tested groups. CA, GPA, AU, and QU represent chlorogenic acid, geniposidic acid, aucubin, and quercetin, respectively

	Control	H_2O_2	H_2O_2 + CA	H_2O_2 + GPA	H_2O_2 + AU	H_2O_2 + QU
Sirt1	519	62.928	131.28	210.67	135.09	108.57
	504.33	56.33	118.66	231.97	149.67	98.84
	533.67	69.53	143.9	189.37	120.51	118.3
p53	95.589	768.81	461.97	338.26	336.33	549.93
	101.38	827	446.39	302.75	307.17	566.5
	89.8	710.61	477.55	373.77	365.49	533.36
p21	380.4	1161.4	1144.4	750.99	685.29	991.19
	299.81	1039.49	1318.25	626.91	529.91	1075.36
	460.99	1283.31	970.55	875.07	840.67	907.02
p16	150.16	1662.9	1204.8	1044	937.49	1199.8
	162.97	1750.565	1145.004	1151.51	862.293	1106.75
	137.35	1575.235	1264.596	936.49	1012.687	1292.85
GAPDH-1	2650	2733.5	2940.8	3019.1	2803.1	2750
P-Rb	185.32	834.97	554.34	410.51	414.43	657.26
	211.56	897.7135	650.26	373.914	380.982	716.128
	159.08	772.2265	493.69	447.106	447.878	598.392
Bcl-2	345	81.226	128.48	152.93	132.61	87.654
	391.35	73.49	155.99	141.58	124.56	121.87
	298.65	88.97	100.97	164.28	140.66	53.43
Bax	267.28	945.5	1022	866.14	970.84	1034
	307.65	1016.462	1092.29	824.012	1025.178	1121.95
	226.91	874.538	951.71	908.268	916.502	946.05
p65	172.5	748.25	909.81	1015.4	998.49	879.61
	151.94	693.239	806.21	894.598	895.21	820.462
	193.06	803.261	801.79	875.34	754.41	975.262
GAPDH-2	3287.3	3356.95	3527	3726.6	3473.6	3650.4
P-ERK	960.77	1549.6	1550.6	1357.6	1444.012	1301
	915.28	1624.769	1653.43	1353.29	1384.359	1178.06
	1006.26	1474.431	1447.77	1361.91	1342.686	1423.94
Survivin	566.13	294.58	392.39	323.71	330.47	268.46
	607.18	322.246	327.7	355.63	276.007	234.904
	525.08	266.914	313.25	291.79	384.933	302.016
GAPDH-3	2152.5	2052.7	2193.8	2310.7	2299.7	2362.8